as in part I.[22] The initial concentration of HF, $C_{HF}$, was corrected for reaction with iodate to give a partially corrected HF concentration, $M_{HF}$

$$M_{HF} = C_{HF} - 2[IO_2F_2^-]$$

Equilibrium molalities of HF in aqueous solutions have been measured up to an initial HF concentration of 4 $m$[23] and [HF] listed in Table III has been evaluated from these data by interpolation and using density data in ref 21, p 54. It was assumed that $\gamma_{HF} = 1$. The [HF] at higher concentrations than 4 $m$ (3.82 $M$) have been arrived at by a linear extension of Hamer and Wu's data.[23] The justification for this procedure comes from Fredenhagen's work[24] where it was shown that the partial pressure of HF over aqueous solutions shows a linear dependence on HF concentration up to above 7.0 $M$. Hydrogen fluoride vapor is known to be monomeric up to vapor pressures above those measured over 7.0 $M$ HF.[25] Water activities have been calculated from $H_2O$ vapor pressure measurements over aqueous HF solutions[24] as was done in previous work.[22] The effect of $HClO_4$, present for peak normalization purposes, and the I(V) anions on [HF] and $a_{H_2O}(N)$ in these solutions has not been taken into consideration. In spite of this, there is satisfactory agreement in $K_h$ over a wide range of $C_{HIO_3}$ and $C_{HF}$ as shown in Table III, solutions 4–8. The hydrolysis constant, $K_h$, was found to be $17 \pm 2$ $m^2$ l.$^{-2}$.

The hydrolysis of I(V) in 24 $M$ HF solutions is much more extensive than that for Te(IV)[22] and Sb(III)[9] under the same conditions. The $TeF_5^-$ ion is observed in 6 $M$ HF while iodine pentafluoride appears in HF solutions only at HF concentrations of $\sim$55 $M$ and above.[9]

**Acknowledgment.** We thank Dr. A. R. Davis for the use of his Raman spectrometer and the National Research Council for financial assistance.

**Registry No.** $CsIO_2F_2 \cdot {}^1/_3H_2O$, 54275-79-5; $Co(NH_3)_6(IO_2F_2)_3 \cdot H_2O$, 54275-81-9; $Cs[H(IO_2F_2)_2] \cdot 2H_2O$, 54275-82-0; $IO_2F_2^-$, 30669-35-3; $HIO_3$, 7782-68-5.

## References and Notes

(1) K. O. Christe, *Inorg. Chem.*, **11**, 1215 (1972).
(2) R. R. Ryan and L. B. Asprey, *Acta Crystallogr., Sect. B*, **28**, 979 (1972).
(3) A. Finch, P. N. Gates, and M. A. Jenkinson, *J. Chem. Soc. A*, 2044 (1972).
(4) J. J. Pitts, S. Kongpricha, and A. W. Jache, *Inorg. Chem.*, **4**, 257 (1965).
(5) R. F. Weinland and D. Koppen, *Z. Anorg. Chem.*, **22**, 256 (1901).
(6) L. Helmholz and M. T. Rogers, *J. Amer. Chem. Soc.*, **62**, 1537 (1940).
(7) H. A. Carter and F. Aubke, *Inorg. Chem.*, **10**, 2296 (1971).
(8) A. Finch, P. N. Gates, and M. A. Jenkinson, *J. Fluorine Chem.*, **2**, 111 (1972).
(9) J. B. Milne and D. Moffett, to be submitted for publication.
(10) A. I. Vogel, "Quantitative Inorganic Analysis," 3rd ed, Longmans, Green and Co., New York, N.Y., 1966.
(11) J. B. Milne and D. Moffett, *Inorg. Chem.*, **12**, 2240 (1973).
(12) H. Siebert, "Anwendungen der Schwingungsspektroskopie in der anorganischen Chemie," Springer-Verlag, Berlin, 1966, p 90.
(13) H. D. Lutz, H. J. Kluppel, and R. Kho, *Angew. Chem., Int. Ed. Engl.*, **10**, 183 (1971).
(14) A. C. Pavia and P. A. Giguere, *J. Chem. Phys.*, **52**, 3551 (1970), and references therein.
(15) P. A. Giguere, *Rev. Chim. Miner.*, **3**, 627 (1966).
(16) W. E. Dasent and T. C. Waddington, *J. Chem. Soc.*, 2429 (1960).
(17) H. H. Classen, E. L. Gasner, H. Kim, and J. L. Huston, *J. Chem. Phys.*, **49**, 253 (1968).
(18) C. J. Adams and A. J. Downs, *J. Chem. Soc. A*, 1534 (1971).
(19) C. J. Adams and A. J. Downs, *Spectrochim. Acta*, **28**, *Part A*, 1841 (1972).
(20) J. R. Durig, O. D. Bonner, and W. H. Breazeale, *J. Phys. Chem.*, **69**, 3886 (1965).
(21) "International Critical Tables," Vol. III, McGraw-Hill, New York, N.Y., 1928.
(22) J. B. Milne and D. Moffett, *Inorg. Chem.*, **13**, 2750 (1974).
(23) W. J. Hamer and Y. Wu, *J. Res. Nat. Bur. Stand., Sect. A*, **74**, 761 (1970).
(24) K. Fredenhagen and N. Wellmann, *Z. Phys. Chem., Abt. A*, **162**, 454 (1932).
(25) K. Fredenhagen, *Z. Anorg. Allg. Chem.*, **218**, 161 (1934).

---

Contribution from the Department of Chemistry, Cornell University, Ithaca, New York 14853

# Molecular Structure of Octadecahedral Carboranes by Gas-Phase Electron Diffraction. 1,2-Dicarba-*closo*-hexaborane(6) and Carbahexaborane(7)

EDWARD A. McNEILL and FRED R. SCHOLER*

*Received September 11, 1974* AIC406432

Gas-phase electron diffraction patterns of 1,2-dicarba-*closo*-hexaborane(6) and carbahexaborane(7) were recorded at room temperature. Least-squares analyses of the reduced intensity data confirm the distorted octahedral geometry of the respective carboranes in the gas phase. The following structural parameters have been obtained for 1,2-$B_4C_2H_6$, $r_g$: C(1)–C(2) = 1.535 Å, C(1)–B(5) = 1.621 Å, C(1)–B(4) = 1.618 Å, B(4)–B(3) = 1.745 Å, and B(3)–B(5) = 1.723 Å. The bond angles are B(5)C(1)B(6) = 96.7°, B(5)B(3)B(6) = 89.4°, and C(1)B(5)B(3) = 86.9°. The angles are measured in terms of $r_\alpha$ and the uncertainties set at $3\sigma$ ($\sigma$ is the least-squares standard deviation). The structural parameters ($r_g$) of $CB_5H_7$ are B(2)–B(3) = 1.921 Å, B(3)–B(4) = 1.685 Å, B(4)–B(5) = 1.756 Å, C(1)–B(2) = 1.602 Å, C(1)–B(4) = 1.659 Å, B(2)–B(6) = 1.909 Å, and B(4)–B(6) = 1.689 Å. The bond distance for the bridging H(7) to B(2) is 1.399 Å and from H(7) to B(6) is 1.397 Å indicating the bridge hydrogen is located at a nearly central position on the B(2)B(3)B(6) face. The bond angles are B(3)C(1)B(2) = 73.7°, B(3)C(1)B(4) = 62.2°, B(4)C(1)B(5) = 63.9°, B(2)B(3)B(6) = 59.8°, B(2)B(6)B(3) = 60.4°, B(2)B(6)B(5) = 55.4°, and B(4)B(6)B(5) = 62.6°. The structural data for the carbahexaborane(7) confirms the structure predicted by low-temperature NMR experiments. Comparisons of the structural data are made with the 1,6-dicarba-*closo*-hexaborane(7).

## Introduction

Both electron diffraction[1–4] and rotation–vibration spectra[5–7] have been valuable in determining the molecular structure, geometric parameters, and vibrational amplitudes of the volatile carboranes and boron hydrides. Because crystalline samples of the more volatile carboranes are difficult to isolate, X-ray crystal analysis has not been used in the area of small carboranes.

In this report we present structural data for the octahedral carboranes 1,2-dicarba-*closo*-hexaborane(6) and carbahex-

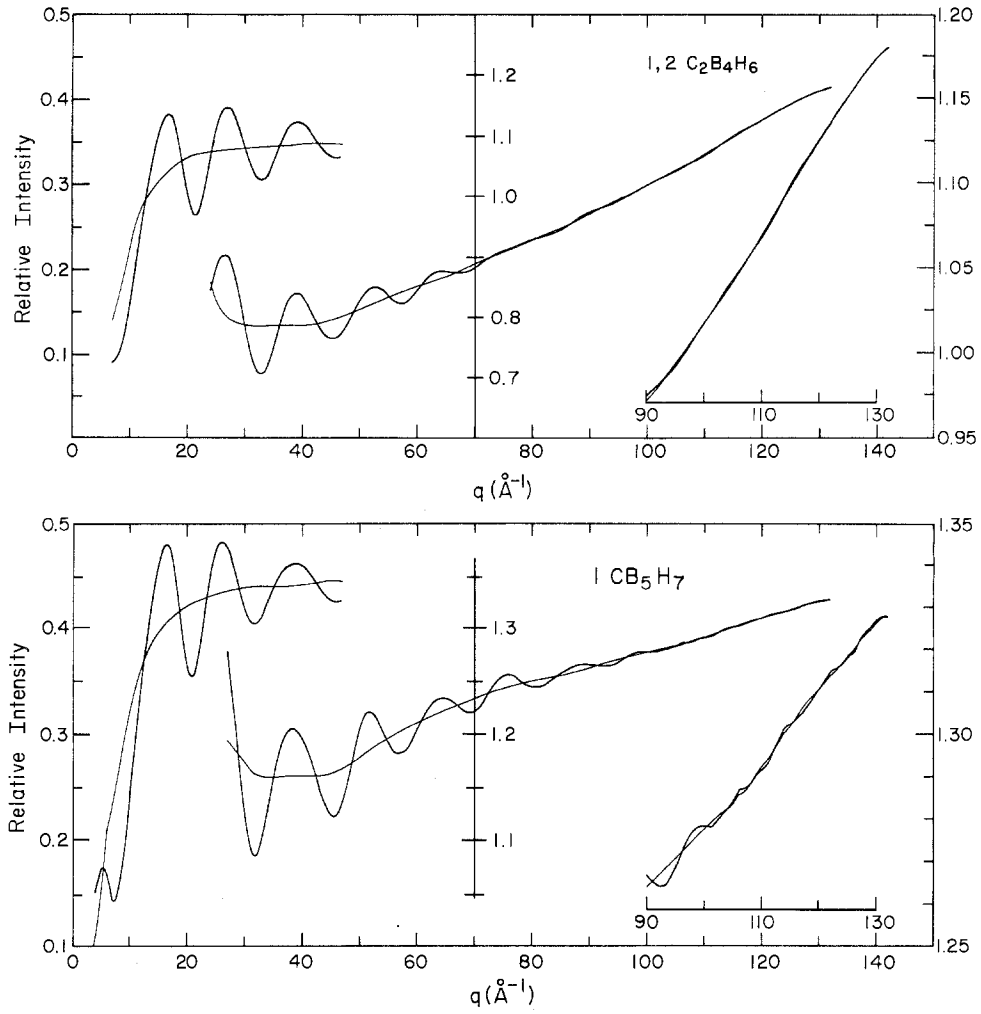


**Figure 1.** Relative scattered intensity and refined background curves for (top) 1,2-$B_4C_2H_6$ (splice point $q = 42$ Å$^{-1}$) and (bottom) $CB_5H_7$ (splice point $q = 35$ Å$^{-1}$).

**Table I.** Geometrical and Thermal Parameters[a]

| 1,2-$B_4C_2H_6$ | | $CB_5H_7$ | | |
|---|---|---|---|---|
| | | | Values | |
| Parameters | Values | Parameters | Model I | Model II |
| o-B(5)[b] | 1.2116 (18) | o-C | 1.0466 (51) | 1.0444 (64) |
| o-D(1) | 0.7556 (48) | o-D(1) | 0.7409 (141) | 0.7513 (133) |
| D(1)-C(1) | 0.7673 (12) | D(1)-B(2) | 0.9607 (39) | 0.9577 (40) |
| o-D(2) | 0.8597 (95) | o-D(2) | 0.9426 (78) | 0.9795 (151) |
| D(2)-B(3) | 0.8729 (48) | D(2)-B(4) | 0.8780 (45) | 0.8380 (66) |
| C-H | 1.1038 (54) | o-B(6) | 1.3206 (36) | 1.3164 (66) |
| B-$H_{ave}$ | 1.2252 (36) | C-H | 1.0911 (84) | 1.0853 (87) |
| ∠o-B(5)-H(11) | 195.0 (2.1) | B-$H_{av}$ | 1.2057 (24) | 1.2072 (24) |
| | | ∠C-o-B(6) | 167.3 (0.7) | 167.0 (0.9) |
| *l*(C-H | 0.094 (10) | D(1)-H(7) | 0.9185 (112) | 0.9222 (101) |
| *l*(B-H) | 0.085 (10) | ∠o-D(1)-H(7) | 109.1 (1.2) | 108.4 (1.2) |
| *l*(C(2)-C(3)) | 0.056 (8) | | | |
| *l*(C(2)-B(5)) | 0.061 (6) | *l*(C-H) | 0.080 | 0.080 |
| *l*(B(1)-C(2)) | 0.058 (6) | *l*(B-$H_t$) | 0.067 (3) | 0.066 (3) |
| *l*(B(1)-B(4)) | 0.058 (6) | *l*(B-$H_b$) | 0.055 (9) | 0.054 (9) |
| *l*(B(4)-B(5)) | 0.056 (12) | *l*(C-B(2)) | 0.069 (1) | 0.069 (1) |
| *l*(C(2)···B(4)) | 0.061 (1) | *l*(C-B(4)) | 0.069 (1) | 0.069 (1) |
| *l*(B(1)···B(6)) | 0.081 (4) | *l*(B(2)-B(5)) | 0.073 (1) | 0.072 (1) |
| | | *l*(B(4)-B(5)) | 0.073 (1) | 0.072 (1) |
| | | *l*(B(6)-B(4)) | 0.073 (1) | 0.072 (1) |
| | | *l*(B(2)-B(3))) | 0.087 (2) | 0.086 (2) |
| | | *l*(B(6)-B(2)) | 0.087 (2) | 0.086 (2) |
| | | *l*(C- - -B(6)) | 0.060 (3) | 0.060 (3) |
| | | *l*(B(2)- - -B(4)) | 0.064 (2) | 0.064 (2) |

[a] Distances are in angstroms; angles are in degrees. The calculated uncertainties are given in parentheses. These uncertainties are 3 times the least-squares standard deviation. [b] Origin indicated by o.

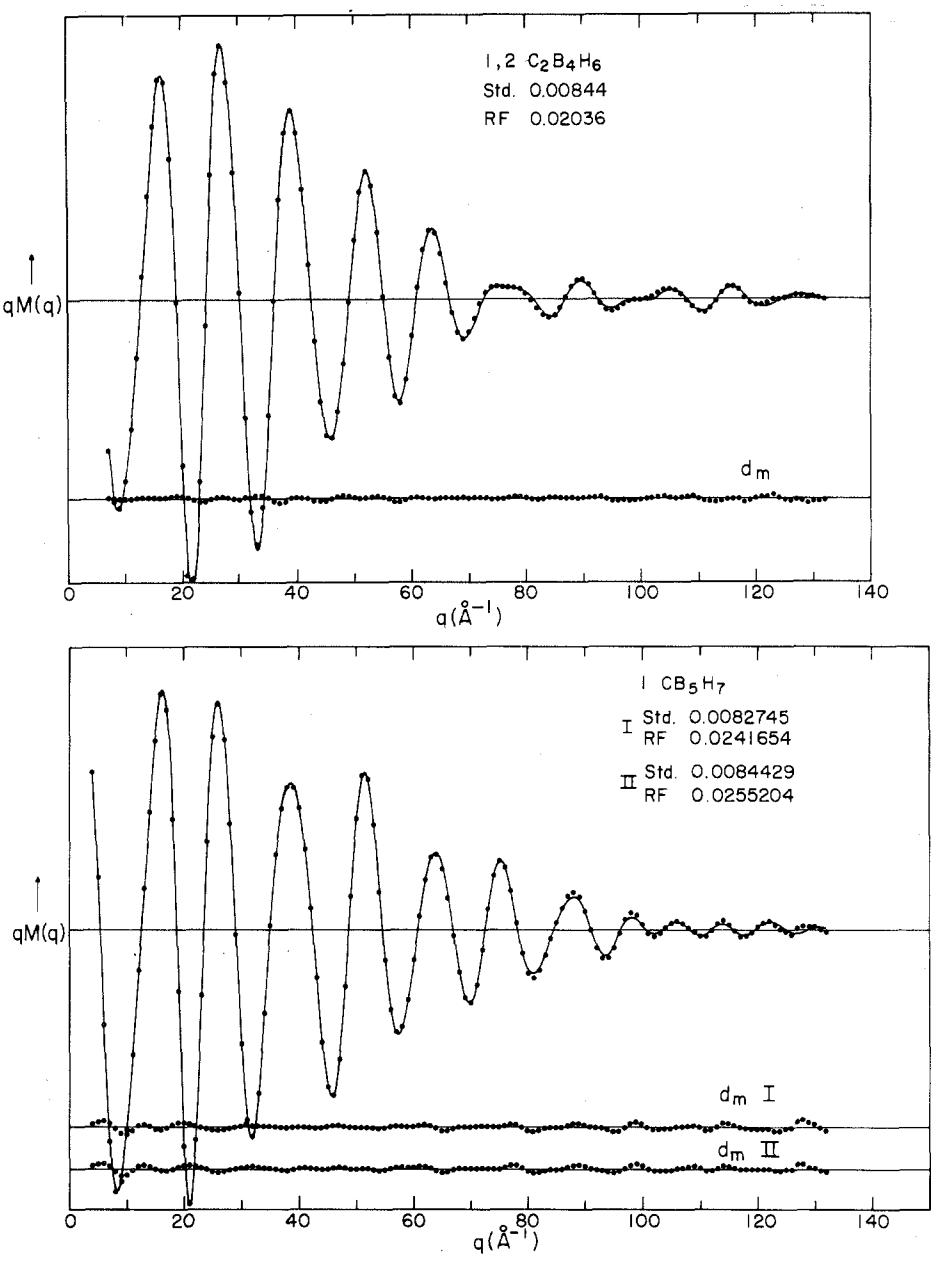


**Figure 2.** The reduced experimental molecular scattering curves, $qM(q)$ (dots), the theoretical $qM(q)$ (solid line), and the dashed difference curve, $d_m$, for (top) 1,2-$B_4C_2H_6$ and (bottom) $CB_5H_7$, where model I and model II difference curves are labeled.

aborane(7) as deduced from electron diffraction patterns in the gas phase. The gas-phase structure of the third member of the octahedral family of carboranes, 1,6-dicarba-*closo*-hexaborane(6), has been previously determined by electron diffraction analysis.[1] The molecular symmetry of carbahexaborane(7) has been analyzed both by temperature-dependent nuclear magnetic resonance studies[8] and by microwave spectroscopy.[9]

## Experimental Section

**1,2-$B_4C_2H_6$.** A sample of 1,2-$B_4C_2H_6$ was prepared by photolysis (214 nm) of a 2:1 mixture of sulfur hexafluoride and 2,3-$B_4C_2H_8$ (18 cm of total pressure). Irradiation of the gas mixture for 2 hr with a low-pressure mercury lamp equipped with a Vycor filter gave 1,2-$B_4C_2H_6$ in over 30% yield based on the amount of 2,3-$B_4C_2H_8$ recovered. This adaptation of the procedure of Spielman and Scott[10] increases the amount of 1,2-$B_4C_2H_6$ isolated by a factor of 3. The sample was purified by repeated passages through an F & M 700 gas chromatograph at 60° on a 3-ft column of 30% Apiezon L on Chromosorb P. Samples prepared by this method were at least 98% pure. The helium carrier gas was removed in vacuo at −196°. The sample was warmed to room temperature and sectored photographs were taken with the Cornell instrument.[11] The sample to plate distance and wavelengths were established for the short nozzle to plate distances by concurrently recording $CO_2$ diffraction patterns and for the long distances by MgO diffraction patterns[12-14] [λ 0.044202 and 0.056519 Å at sample to plate distances of 127.4 mm ($q$ = 24–132 Å$^{-1}$) and 284.9 mm ($q$ = 7–47 Å$^{-1}$), respectively, where $q = (40/\lambda)(\sin\theta)/2$]. All patterns were recorded on 4 × 5 in. Kodak Electron Image plates. The radial optical density functions for the diffraction data were obtained with a double-beam Jarrel-Ash densitometer, interfaced with a digital recorder. Four data sets were taken for each distance. These were converted to relative intensities, interpolated at integral values of $q$, corrected for nonflatness of the focal plane, and averaged.

**$CB_5H_7$.** The sample of $CB_5H_7$ was prepared according to the procedure by Onak et al.[10] The sample was purified by repeated passages through an F & M 700 gas chromatograph at 90° on a column of 30% Apeizon L on Chromosorb P. Sectored patterns were recorded with wavelengths of 0.056519 and 0.044202 Å at sample to plate distances of 287.2 mm ($q$ = 4–47 Å$^{-1}$) and 127.3 mm ($q$ = 27–132 Å$^{-1}$), respectively. MgO and $CO_2$ diffraction patterns were taken concurrently to establish the long and short nozzle to plate distances, respectively. Six short and four long data sets were collected, processed, and averaged. The procedure for structural analysis has been described elsewhere.[15-17]

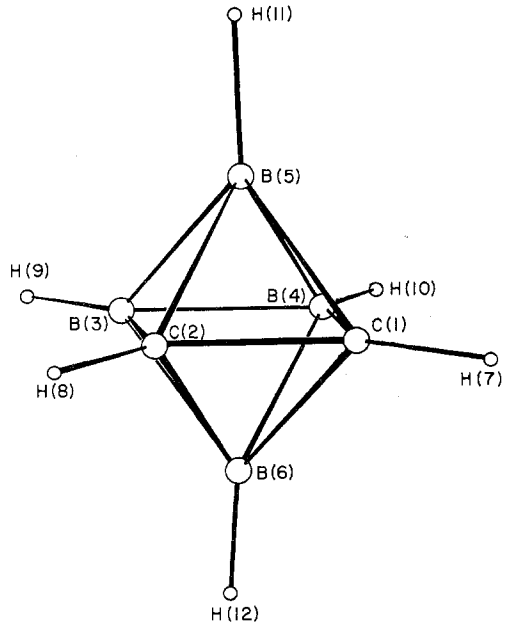


Figure 3. Molecular structure and numbering scheme for 1,2-$B_4C_2H_6$.

## Results

**1,2-$B_4C_2H_6$.** Figure 1 is a plot of relative scattered intensity as a function of the angle [$q$ (Å$^{-1}$)] with a refined background. The reduced scattered intensity [$qM(q)$] as a function of $q$ (Å$^{-1}$) is shown in Figure 2. The atomic configuration and numbering scheme is given in Figure 3. The $z$ axis is collinear with atoms B(5) and B(6). The $x$ axis bisects both the C(1)–C(2) and B(3)–B(4) bonds. The $y$ axis is mutually perpendicular to the $xz$ plane and intersects the C(1)–B(4) bond. In order to facilitate the parameterization of the 1,2-$B_4C_2H_6$ two "dummy atoms" D(1) and D(2) were placed on the $x$ axis at the midpoints of the C(1)–C(2) and B(3)–B(4) bonds, respectively. The eight geometric parameters required to specify the coordinates of the atoms are the distances from the origin to B(5), the origin to D(1), the origin to D(2), D(1) to C(1), and D(2) to B(3), the angle defined by origin–B(5)–H(11), and the average B–H distance and the C–H distance. The terminal hydrogens, except for H(11), were set to bisect the external angles. The B(5)–H(11) bond is in the $xz$ plane but not parallel with the $z$ axis (*vide infra*).

The longer nonbonded vibrational parameters, $l_{ij}$, beyond 2.75 Å, were held fixed during least-squares refinement but were continuously estimated from trial radial distribution curves. In the final least-squares refinement of the $qM(q)$ curve all geometric parameters, except for the angle defined by the origin–B(5)–H(11), were varied as well as five cage bonded $l_{ij}$'s and four cage nonbonded $l_{ij}$'s. The terminal hydrogen $l_{ij}$'s were held constant. The final standard deviation and $R$ factor were 0.00844 and 0.02037, respectively.[18]

The radial distribution curve shown in Figure 4 was obtained after a series of refinements of the background. The difference between the experimental and the "best" model curves is denoted in Figure 4 by the lower line $d_f$. In the radial distribution curve the atom–atom pair distances are indicated by vertical lines and the height of each was made proportional to the theoretical peak height. Values for the geometrical parameters and the root-mean-square amplitudes were refined in a series of least-squares calculations to match the $qM(q)$ curve. The best set of geometric and thermal parameters for the 1,2-$B_4C_2H_6$ is summarized in Table I.

The H(11) atom is constrained to be in the $xz$ plane but is not collinear with the $z$ axis. In the radial distribution curve two peaks occur at 2.734 Å assigned to the nonbonded atom–atom pair H(11)–C(2) and at 2.606 Å assigned to H(11)–B(3). If H(11)–C(2) were collinear with the $z$ axis, these two peaks would converge. The "best" fit has the H(11) atom in the $xz$ plane approximately 15° away from the $z$ axis in the direction of atoms B(3)–B(4). The $z$ coordinate for H(11) is then 1.184 Å, which compares favorably with the value of 1.183 Å calculated from its microwave spectrum. The moments of inertia based on this model system agree within 1% with those obtained by microwave spectroscopy.

**$CB_5H_7$.** The optical density data were evaluated and processed in the same manner described for 1,2-$B_4C_2H_6$ and plotted as a function of the scattering angle, along with a refined background in Figure 1. The $qM(q)$ curve is shown in Figure 2. As with 1,2-$B_4C_2H_6$ two "dummy atoms," D(1) and D(2), were added midway between atoms B(2)–B(3) and B(4)–B(5), respectively. The atomic configuration and the numbering scheme is shown in Figure 5. The $z$ axis is collinear with the C(1)–B(8) atom pair. The $x$ axis bisects the atom pair B(2)–B(3) and its intersection with $z$ defines the origin and $y$ axis. Eleven geometrical parameters are required to specify the atom positions: the distances from the origin to C(1), the origin to D(1), the origin to D(2), D(1) to B(2), D(2) to B(4), the origin to B(6), and the bridging hydrogen H(7) to D(1), the angles defined by C(1)–origin–B(6) and origin–D(1)–H(7), and the C–H distance and the average B–H

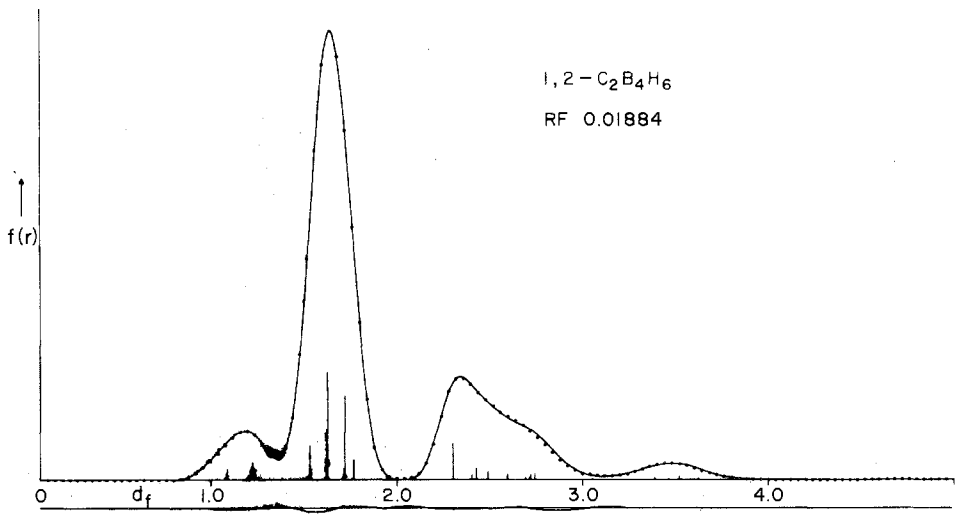


Figure 4. The refined experimental radial distribution curve (dots), the theoretical radial distribution curve (solid line), and the difference curve, $d_f$, for 1,2-$B_4C_2H_6$.

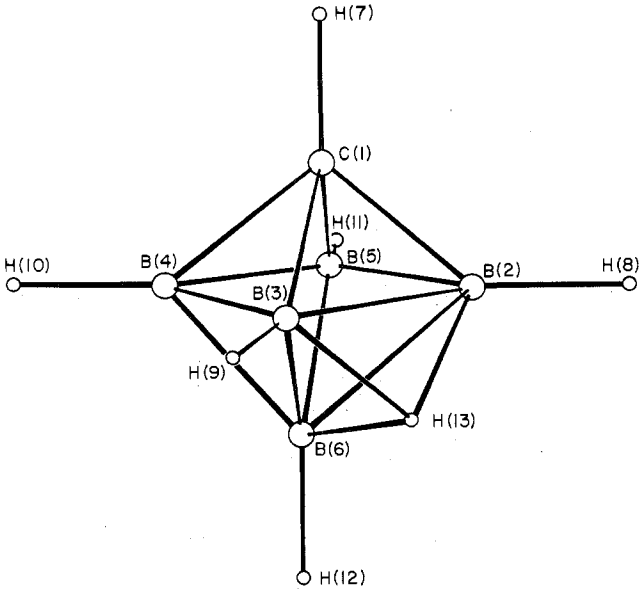


Figure 5. Molecular structure and numbering scheme for $CB_5H_7$.

distance. The B(6)–H(12) atom pair is kept parallel to the $z$ axis and the bridging hydrogen, H(7), is kept on the $xz$ plane. The other terminal hydrogens were set to bisect the external angles.

The longer nonbonded vibrational parameters, $l_{ij}$'s, were held fixed in the least-squares refinement but were continuously estimated from trial radial distribution curves. The shorter $l_{ij}$'s were varied in the final least-squares refinement of the $qM(q)$ curve. In all cases in the least-squares refinement the eight geometrical parameters and the ten $l_{ij}$'s were varied independently. The final stages of refinement indicated two models, I and II, were compatible with the electron diffraction data. The final standard deviation and $R$ factor were 0.00844 and 0.02552 for model II and 0.00827 and 0.02416 for model I.

The $qM(q)$ curve along with the difference curves for models I and II is shown in Figure 2. The two difference curves are virtually indistinguishable. The two radial distribution curves for models I and II shown in Figure 6 were obtained after a series of refinements of the background. The difference between the experimental and the "best" model curves is denoted by the lower line $d_f$.

Two features of relative importance are noted in the radial distribution curves. For both models the peak at 2.17 Å is assigned to the C(1)–H(7) nonbonded interaction. H(7) was kept in the $xz$ plane and the nonbonded distance allowed to vary. For both models this particular geometric parameter establishes the bridging hydrogen as being located near the center of the triangle of atoms B(2), B(3), and B(4). Figure 7 is a projection down the pseudo $C_3$ axis. The third and fourth peaks in the radial distribution curve at 1.32 and 1.39 Å are

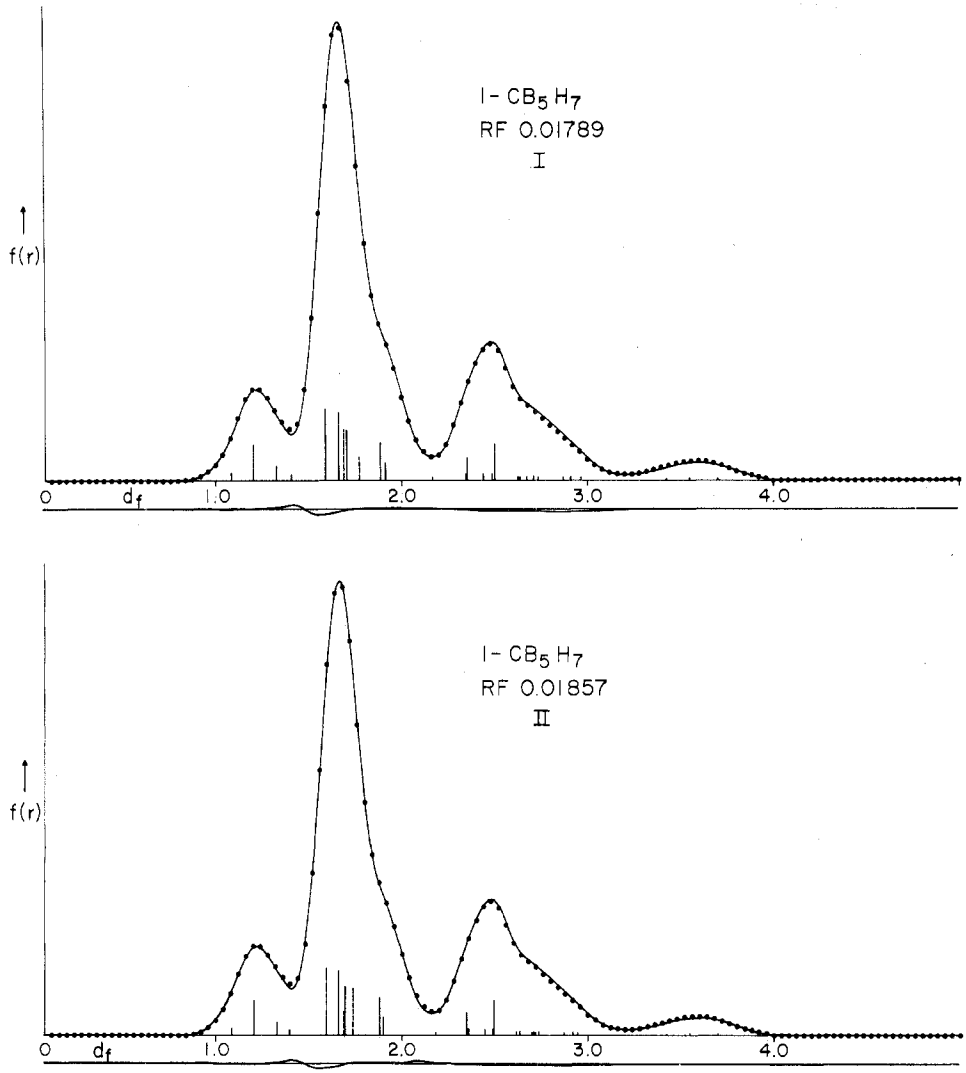


Figure 6. The refined experimental radial distribution curve (dots), the theoretical radial distribution curve (solid line), and the difference curve, $d_f$, for (top) model I and (bottom) model II, for $CB_5H_7$.

Table II. Atom Pair Distances (Å) and Angles (deg)

| $1,2\text{-}B_4C_2H_6$ | | $CB_5H_7$ | | |
|---|---|---|---|---|
| | | | Model I | Model II |
| | | Bonded Distances | | |
| C-H | 1.104 (5) | C-H | 1.091 (8) | 1.085 (8) |
| $B\text{-}H_{av}$ | 1.225 (4) | $B\text{-}H_t$ | 1.206 (2) | 1.207 (3) |
| C(1)-C(2) | 1.535 (2) | B(2)-H(7) | 1.329 (16) | 1.329 (16) |
| C(2)-B(3) | 1.618 (14) | B(6)-H(7) | 1.397 (19) | 1.399 (19) |
| C(1)-B(5) | 1.621 (4) | C(1)-B(2) | 1.602 (6) | 1.604 (6) |
| B(3)-B(5) | 1.723 (8) | C(1)-B(4) | 1.660 (6) | 1.659 (6) |
| B(3)-B(4) | 1.745 (10) | B(3)-B(4) | 1.686 (18) | 1.735 (22) |
| | | B(3)-B(6) | 1.690 (8) | 1.678 (8) |
| | | B(4)-B(5) | 1.756 (9) | 1.676 (12) |
| | | B(2)-B(6) | 1.910 (11) | 1.913 (13) |
| | | B(2)-B(3) | 1.921 (8) | 1.915 (8) |
| | | Nonbonded Distances | | |
| C(1)- - -B(3) | 2.302 (7) | C(1)- - -B(6) | 2.353 (8) | 2.346 (9) |
| B(5)- - -B(6) | 2.423 (4) | B(2)- - -B(4) | 2.493 (5) | 2.494 (5) |
| | | Angles | | |
| | | C(1)B(2)B(6) | 83.6 (9) | 83.2 (9) |
| B(5)C(1)B(6) | 96.7 (0.9) | C(1)B(4)B(6) | 89.2 (9) | 89.3 (9) |
| B(5)B(3)B(6) | 89.4 (1.4) | B(2)B(6)B(4) | 87.5 (9) | 87.7 (8) |
| C(1)B(5)B(3) | 86.9 (0.9) | B(2)C(1)B(4) | 99.7 (7) | 99.7 (7) |

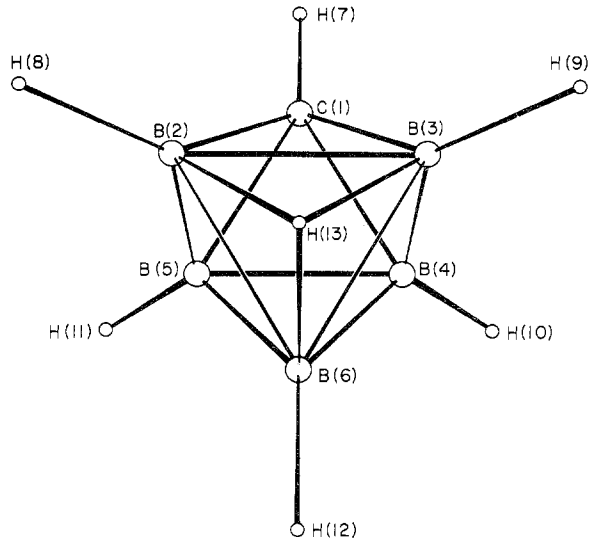


Figure 7. Projection of $CB_5H_7$ down the pseudo threefold axis defined by atoms B(2)B(3)B(6).

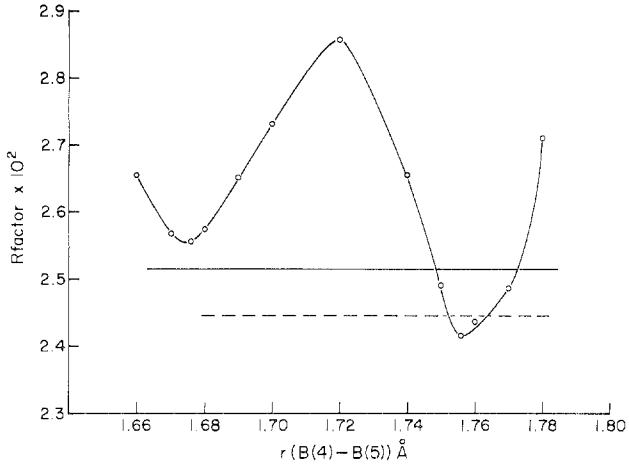


Figure 8. Plot of $R$ factor vs. B(4)-B(5) distance where the two horizontal lines refer to the 99.5% (dashed line) and 95.0% (solid line) confidence intervals with Hamilton's ratio of $R$ factors equal to 1.041 and 1.019, respectively.

assigned to the B(2)–H(7) and B(6)–H(7) bonded interaction. The $l_{ij}$'s chosen initially for H(7) were based on comparative values for the pentaborane(9) structure.

Models I and II differ primarily with respect to the shape of the trapezoid defined by atoms B(2), B(3), B(4), and B(5). In model I the bond distance B(4)–B(5) is longer (1.756 Å) than B(4)–B(3), 1.685 Å. The respective values for model II are 1.676 and 1.735 Å. These variations are noted in the radial distribution curve by dashed lines. The $R$ factor and standard deviation favor model I slightly (0.02416 and 0.00827 for I; 0.02552 and 0.00844 for II). Application of Hamilton's ratio of $R$ factors ($R$) to test the significance of these results[19] reveals a double minimum in the plot of $R$ factor vs. B(4)–B(5) bond length (Figure 8). A 95% confidence limit confines the B(4)–B(5) bond length to 1.752 and 1.765 Å. From our model I the best fit distance is 1.756 Å. Based on the final internuclear distances and bond angles for the two models (Table II) the moments of inertia can be calculated. For model I the moments of inertia $I_x$ are consistently larger than $I_y$. In model II the values for $I_y$ are consistently larger than $I_x$. Comparison of the calculated vs. the experimental values for the moments of inertia as derived from the rotational–vibrational spectra should resolve this problem. Values for the geometrical parameters and the root-mean-square amplitudes were refined in a series of least-squares calculations to match the $qM(q)$ curve for both models and are shown in Table I. We favor model I over model II.

## Discussion

The structural data for $1,2\text{-}B_4C_2H_6$ are found in Table II and the molecular structure is shown in Figure 3. The structural data from this study are consistent with those reported by Beaudet and Poytner[5] from the microwave study. The B–B bond lengths and B–C bond lengths obtained in this study, Table II, and those for $1,6\text{-}B_4C_2H_6$, Table II in ref 1, compare favorably. The B–B nonbonded distances between opposite vertices are nearly equal (2.423 vs. 2.401 Å, respectively). The $qM(q)$ curves for both $1,2\text{-}B_4C_2H_6$ and $1,6\text{-}B_4C_2H_6$ are nearly identical to approximately $90q$ ($Å^{-1}$). These correspond to the nonbonded interactions and affirm the general octahedral features of the 1,2- and $1,6\text{-}B_4C_2H_6$.

For an exact interpretation of molecular structure the combination of rotation and rotation–vibration spectroscopy and gas-phase electron diffraction is often a necessity. In $1,2\text{-}B_4C_2H_6$ the C(2)–B(3) bond length determined by electron diffraction (1.618 ± 0.01 Å) has a high degree of uncertainty. Referring to the radial distribution curve, Figure 4, the peak at 1.618 Å is assigned to the atom pair C(2)–B(3). The

uncertainty arises from the proximity of this peak to the more intense C(1)–B(5) peak. In the microwave study the consistency of results is excellent for those bond lengths, which are unaffected either by an atom being on the principal axis or by a large rotation of the axes upon isotopic substitution,[5] such as C(2)–B(3). The bond distance, C(2)–B(3), from the microwave structure is 1.605 ± 0.005 Å.

For the B(5) atom, which is near the principal *a* axis, its *b* and *c* coordinates are not easily determined by microwave spectroscopy. The B(5)–B(4), 1.721 ± 0.015 Å, and B(5)–C(1), 1.627 ± 0.015 Å, have comparatively large uncertainties. The corresponding bond lengths determined by electron diffraction are 1.723 ± 0.008 and 1.621 ± 0.004 Å. When both rotational constants and diffraction intensities are simultaneously available, the gas-phase structure can be more accurately determined and resolve the problem of closely spaced internuclear distances so often encountered in electron diffraction.

The molecular structure of the carbahexaborane(7) has been established as a distorted octahedron, Figure 5. Referring to Table II many of the structural parameters for the 1,2-$B_4C_2H_6$, 1,6-$B_4C_2H_6$, and $CB_5H_7$ are quite similar. As in the 1,2-$B_4C_2H_6$ and 1,6-$B_4C_2H_6$ the $qM(q)$ curves are all comparable out to $90q$ (Å$^{-1}$). Onak et al. have noted the common octahedral geometry found for these three carboranes is reflected in the similar range of chemical shift values obtained in the $^1H$ and $^{11}B$ NMR spectra.[8] The most unusual structural feature of $CB_5H_7$ is the location of the bridging hydrogen. In order to determine a unique structure for $CB_5H_7$, data were collected to $132q$ (Å$^{-1}$). We were unable to assign hydrogen positions based on data collected to only $100q$ (Å$^{-1}$). Figure 7 is a projection of the bridge hydrogen H(7) upon the pseudo-threefold face of the octahedron B(2)B(3)B(6). This is consistent with the $^1H$ and $^{11}B$ NMR results found by Onak and "would allow the tautomeric hydrogen to follow a path with little deviation from an appropriately placed imaginary plane just below the equatorial boron atoms." The B(2)–H(7) distance of 1.328 Å and the B(6)-H(7) distance of 1.398 Å are consistent with the boron–hydrogen distance in other bridge bonds. The nearly equivalent distances of H(7) from either B(2), B(3), or B(6) indicates the bridging hydrogen is bound to all three borons, which may account for the very low vibrational amplitude of 0.057 Å for H(7). The value for the bridging hydrogen in pentaborane(9) is 0.085 Å. The placement of the H(7) atom in a position considerably closer to B(6) would then permit tautomeric movement of the bridge hydrogen around the octahedra with intermediate positions at the B(3)–B(6) edges.

In the generation of $CB_5H_7$ from the corresponding $CB_5H_6^-$, the $H^+$ would seek the maximum point of electron density on the polyhedral face. Armstrong et al. using self-consistent field molecular orbital calculations on highly symmetrical cage anions, i.e., $B_6H_6^{2-}$, revealed that the electron density builds up inside the cage and reaches a maximum at the center and on the trigonal faces.[20] Since carbon is more electronegative than boron, the $H^+$ ion would seek out the B(2)B(3)B(6) trigonal face.

**Registry No.** $SF_6$, 2551-62-4; 2,3-$B_4C_2H_8$, 21445-77-2; 1,2-$B_4C_2H_6$, 20693-68-9; $CB_5H_7$, 54423-77-7.

## References and Notes


(1) E. A. McNeill, K. L. Gallaher, F. R. Scholer, and S. H. Bauer, *Inorg. Chem.*, **12**, 2108 (1973).
(2) E. A. McNeill and F. R. Scholer, submitted for publication in J. *Mol. Struct.*
(3) R. K. Bohn and M. D. Bohn, *Inorg. Chem.*, **10**, 352 (1971).
(4) V. S. Mastryukov, L. V. Vilkov, A. F. Zhigach, and V. N. Siryatskaya, *Zh. Strukt. Khim.*, **12**, 1081 (1971); **10**, 136 (1969); **7**, 883 (1966).
(5) R. A. Beaudet and R. L. Poynter, *J. Chem. Phys.*, **53**, 1899 (1970).
(6) C. S Cheung and R. A. Beaudet, *Inorg. Chem.*, **10**, 1144 (1971).
(7) R. W. Jotham and D. J. Reynolds, *J. Chem. Soc. A*, 3181 (1971).
(8) E. Groszek, J. B. Leach, G. T. F. Wong, C. Ungermann, and T. Onak, *Inorg. Chem.*, **10**, 2770 (1971).
(9) R. A. Beaudet, paper presented at the Second International Meeting on Boron Chemistry, University of Leeds, Leeds, England, March 1974.
(10) J. R. Spielman and J. E. Scott, *J. Amer. Chem. Soc.*, **87**, 3512 (1965).
(11) S. H. Bauer and K. Kimura, *J. Phys. Soc. Jpn.*, **17**, 300 (1962).
(12) R. L. Hilderbrandt and S. H. Bauer, *J. Mol. Struct.*, **3**, 325 (1969).
(13) Y. Murata, K. Kuchitsu, and M. Kimura, *Jpn. J. Appl. Phys.*, **9**, 591 (1970).
(14) S. H. Bauer, R. R. Karl, and K. L. Gallaher.
(15) W. Harshbarger, G. Lee, R. F. Porter, and S. H. Bauer, *Inorg. Chem.*, **8**, 1683 (1969).
(16) A. L. Andreassen, D. Zebeleman, and S. H. Bauer, *J. Amer. Chem. Soc.*, **93**, 1148 (1971).
(17) A. L. Andreassen and S. H. Bauer, *J. Phys. Chem.*, **76**, 3099 (1972).
(18) $R = |I_{obsd} - I_{calcd}|/|I_{calcd}|$; $I_{obsd}$ is the observed intensity and $I_{calcd}$ is the calculated intensity.
(19) W. C. Hamilton, *Acta Crystallogr.*, **18**, 502 (1965).
(20) D. R. Armstrong, P. G. Perkins, and J. P. Stewart, *J. Chem. Soc. A*, G27 (1973).


---

Contribution from the Department of Chemistry,
Cornell University, Ithaca, New York 14850

# Ion–Molecule Chemistry of $BF_3$ and $HBF_2$ in Hydrogen

ROBERT C. PIERCE and RICHARD F. PORTER*

*Received September 27, 1974* AIC406782

Comparative proton affinity studies indicate that $HBF_2$ and $BF_3$ are protonated by $H_3^+$ but not by $CH_5^+$. Boundaries on the proton affinities of these fluoroboranes are set at 5.10 ± 0.40 eV. At low temperatures near 80°K clustering reactions of $BF_2^+$ occur with formation of the complexes $BF_2{\cdot}H_2^+$ and $BF_2{\cdot}2H_2^+$. In the $BF_3$–$H_2$ system a low-temperature complex $BF_3H{\cdot}H_2^+$ is observed. Third-order rate constants for these clustering reactions have been measured. Physical evidence and theoretical calculations indicate that the species $BF_2{\cdot}H_2^+$ formed by a cluster reaction is structurally distinguishable from $H_2BF_2^+$ formed by proton transfer to $HBF_2$. The species $BF_2{\cdot}2H_2^+$ and $BF_3H{\cdot}H_2^+$ can be treated as four-coordinate structures if each $H_2$ is counted as one unit three-center bonded to the boron atom.

## Introduction

In recent years there has been an increased interest in the kinetic and thermodynamic aspects of proton-transfer reactions in the gas phase. An impetus to this research has been the development of new mass spectrometric techniques including ion cyclotron resonance and chemical ionization which have been used extensively in studies of organic molecules. We have applied the chemical ionization technique to studies of a series of boron hydride molecules and have observed some relationships between basicity (proton affinity) and structure.[1] The original motivation for the experimental work described in the present paper was to obtain a quantitative measure of the basicity of $BF_3$ which is chemically important as a strong Lewis acid in solution. The experiments have revealed an interesting